MILLIMETER ARRAY
MEMO NO. 106

A Slant-Axis Antenna for the MMA:

Computer Simulation Results of Fast Switching

Jingquan Cheng

January 10, 1994

Abstract

The slant-axis antenna is being considered as a possible antenna for the NRAO MMA. For MMA phase calibration in the presence of atmospheric path length fluctuations, the ability to switch the antenna pointing rapidly between the source and a known calibrator may be extremely important. Because of its low moment of inertia, and because the structure is inherently very stiff, the slant-axis antenna may be particularly advantageous in this respect. This memo describes some simulations of fast antenna switching using a computer model of the slant-axis antenna. The time dependent structural displacements have been analyzed. There are two main effects: pointing errors and dish deformation. The conclusion is that the major problem is the pointing errors, resulting from oscillatory movements of the secondary mirror support.

1. Introduction

A fundamental limitation when switching rapidly between positions is the time varying pointing errors caused by structural vibrations that continue after the axis encoder system indicates that the antenna has reached the desired position.

A transient analysis of fast switching on a computer model of a slant-axis antenna has been performed using the Nastran program. All antenna structural components above the slant axis (see Figure 1) were included in the simulation. These components are: the secondary mirror, its support trusses (i.e. the tripod), the panels (weight only), the backup structure (including the mass of all structure joints), the shell-like dish support structure and the slant bearing ring.

The support structure is made of a steel shell which has a thickness of 1 cm. A rigid bearing ring is assumed but the bearing weight is not included in the analysis model. The tripod used in the analysis is a rigid design but has a larger indirect aperture blockage; this tripod raises the natural frequency of the whole structure.

The complete model weighs 4.5 tons. Its center of gravity is about 40 cm above the intersection of the slant bearing and the dish axes. The structure is not fully balanced, but since this analysis excludes gravitational effects, the lack of balance has no effects on the results derived.

The model analyzed has the following first 30 natural frequency modes (Hz):

17.2	17.8	24.1	24.4	25.7	25.9	32.0	32.3	32.5	33.2
41.0	42.3	42.3	50.7	50.7	55.7	57.8	59.2	61.9	66.0
66.1	70.9	72.2	72.2	73.2	75.0	76.3	76.8	77.7	77.9

The analysis is a so-called enforced displacement one, where a large moment of inertia is used at the central grid of the slant bearing.

2. Fast switching routines for analysis

Three switching routines are used in the analysis. These simulate: (a) uniform velocity, (b) uniform acceleration and (c) an exponential displacement. The average distance from a given astronomical source to a nearby calibration source is assumed to be 1.5 degrees. In the analysis, we define time t=0 to be the instant at which the stationary telescope begins to move to a new position 1.5 degrees away.

(a) Uniform velocity. From time t=0, the antenna rotates about the slant axis at a uniform rate, reaching its destination 1.5 degrees away at t=0.5 seconds. The slewing rate is 3 degrees per second. When the antenna stops, strictly speaking the model assumes infinite acceleration for an infinite short time, but this corresponds to a finite impulse, and is a standard technique in analysis of this type.

(b) Uniform acceleration. Starting from t=0, the antenna rotates with uniform acceleration for 0.4 seconds, at which point it has travelled 0.75 degrees. It then reverses its acceleration for another 0.4 seconds and stops at its final position at t=0.8 seconds.

(c) Exponential displacement. From $0 < t < 0.8$, the antenna rotational displacement is calculated by the following exponential function:

$$\theta = 0.2618[1-e^{-t/0.106}]$$

The antenna reaches within 1.5 degrees of its destination at t=0.8 seconds.

For the calculations, the time interval used is 0.01 second

and the displacements are recorded at every two time intervals. The Nastran analysis provide all the grids' displacements and members' strains at each time step. At this stage, only displacements of the 96 dish surface grid nodes and of the secondary mirror nodes are recorded and analyzed.

In the computer simulation, different structural damping factors are applied. Damping factor is a structural parameter which describes the energy loss during structural vibration. If X_1 and X_2 are vibration amplitudes of two successive cycles, the damping factor ξ is defined by the following formula:

$$\frac{2\pi\xi}{\sqrt{1-\xi^2}} = \ln\frac{X_1}{X_2}$$

Damping factor of steel structure is small. A typical value is about 0.02. In the computer simulation, the damping factors used are 0.0, 0.04, 0.06 and 0.10 respectively. The damping factors applied are frequency related. Their value has been adjusted by the program specially for the first mode of vibration (that is 17.2 Hz for the model analyzed) and the practical damping will increase proportionally as the frequency increases.

3. Dish surface deformation during fast switching

3.1 Uniform velocity routine

If the damping factor is zero, after the antenna stops at t=0.5 seconds, the dish surface nodes will continue to vibrate indefinitely. The edge of the dish has an oscillation amplitude of about 1 mm (Fig. 2). The frequency of vibration is about 17.2 Hz, which is the first mode of the structural vibration. From the contour maps of the dish surface, the dish shows a periodically swinging pattern around the slant bearing axis. The deformation of the dish is far worse than the surface accuracy requirement.

If the damping factor is 0.04, the amplitude of vibration at the edge of the dish reduces rapidly with time (Fig. 3a). From the figure, the frequency of the node vibration is also 17.2 Hz. The amplitude of the vibration will reduce to under 100 microns at time t=1.0 seconds. Fig. 3b is the surface contour when the edge of the dish has a peak vibrational displacement at time t=1.02 seconds. At this moment, the dish surface nodes all move to one side in the z direction; the displacements of most surface nodes are about 30 microns. Fig. 3c and 3d show the contour maps in the other two co-ordinates. In these two directions both contour maps show deformations of opposite sign at the top and bottom halves of the dish. The deformations in the y direction (along the dish axis) are larger than those in x direction.

3.2 Uniform acceleration routine

If the damping factor is 0.04, a uniform acceleration routine gives lower excitation to the antenna structure, as seen from Fig. 4. Fig. 4 is diagram of the displacements of the dish edge in the z direction at different times. From the diagrams, the amplitudes of the edge node displacements are well below 100 microns at t=1.0 seconds. The largest displacement in the z direction at the t=1.0 seconds is only 32 microns.

3.3 Exponential displacement routine

If the damping factor is 0.04, an exponential displacement routine has a similar effect to the uniform acceleration one. Fig. 5 shows the displacements of the dish edge in the z direction at different times. The amplitude of vibration is also well below 100 microns after t=1.0 seconds. From the diagram, it can be found that the amplitude will reach 20 microns at the t=1.3 seconds.

4. Secondary mirror nodes' displacement

4.1 Uniform speed routine

In the antenna structural model, two grid nodes are located at the secondary mirror axis: one is at the lower end and the other is at the upper end. The analysis shows that the vibration pattern of both two grid nodes are nearly identical. This suggests that the secondary mirror will point away periodically from the destination position. Differing from the displacements of the dish surface nodes, the displacements of the secondary mirror nodes represent pointing error instead of the degradation of the antenna radiation pattern. In most cases, pointing accuracy is more important than the efficiency of the antenna. If the pointing error is large, the radiation received will be irrelevant either to calibrator or to the source.

When the damping factor is zero, the displacement of the secondary mirror grid point is shown in Fig. 6. From this figure, a pointing error due to the movement of the secondary mirror is 65 arc seconds. This figure is calculated by assuming the whole antenna structure vibrates in a same pattern, therefore the magnification factor of the secondary mirror movement is not considered.

When the damping factor is 0.02, the displacements of the same grid point are shown in Fig. 7a. The amplitude of the grid point vibration is 16 arc seconds at t=1.0 second. After the damping factor is increased to 0.04, the results are shown in Fig. 7b. From this figure, the amplitude of the grid point vibration is 9 arc seconds. Fig. 7c shows the results when the damping factor is 0.06 and Fig.7d is the results when the damping factor is 0.10.

If the pointing error allowed is 3 arc seconds, the settling

time for the secondary mirror (including the slewing time) will be about 2 seconds for a damping factor of 0.02; about 1.3 seconds for a damping factor of 0.04, about 1.0 second for a damping factor of 0.06 and about 0.8 seconds for a damping factor of 0.10.

The relationship between the damping factor and the settling time is shown in Fig. 8.

4.2 Other routines

By applying other routines, the settling time required is improved when the damping factor is not very large. The analysis has been carried for the cases when the damping factors are 0.04, 0.06 and 0.1 respectively. All the results are shown in Fig. 8. For the uniform acceleration case, the results are marked as dots and for the exponential displacement, the results are marked as small crosses. The large settling time of these two cases when the damping factor is 0.10 is due to a longer traveling time of these routines in order to reducing the slewing rate.

5. Discussion

5.1 Frequency estimation of fast switching excitation

Structural vibration is caused by outside excitation. However, in the frequency domain, the excitation is not uniformly distributed. For a routine of a uniform velocity, the excitation applied to the structure is a sharp pulse function(an infinite acceleration). The spectrum of this sharp pulse function covers all the frequency range (in fact when the analysis is performed, Nastran program expands the pulse function over a very small time interval, so the acceleration is finite and the spectrum curve in frequency domain will die out as frequency goes up). By applying this routine, the impact to the structure is larger, but the maximum slewing rate (about 3 degrees per second for the first routine) is the lowest for the fast switching performance.

The simulation of a uniform acceleration corresponds a square pulse function with a large time span. Since the time spent for the pulse is 0.4 seconds, the first few minima of the spectrum in frequency domain are located at the frequencies of 2.5 Hz, 5 Hz, 7.5 Hz..., the dominant excitations are all far away from the natural frequency modes of the slant axis antenna structure. The impact of the excitations to the structure is smaller. But the maximum slewing speed(about 7.5 degrees per second) needed is larger than that in the uniform displacement routine. For the third simulation discussed, the excitation force has the same exponential term as displacement, its spectrum in the frequency domain is therefore limited in a smaller band. The dominant excitation is within 1.5 Hz. This case has the smallest impact on the structure. However, the exponential routine will reach the target position at t=infinite, so deviation from exponential routine has been applied between t=0.75 and t=0.8 seconds. The maximum slewing rate for the

exponential displacement routine is the largest (about 11.3 degrees per second).

From the vibration point of view, the exponential routine is the best one and the uniform acceleration is next favorable. Both routines require a smaller acceleration during fast switching. Co nsequently a lower drive torque is required for the system. However a tradeoff has to be considered to avoid higher strain level buildup in the antenna members. High member strain level will cause failure of members after year round switching operation. Member strain level is caused by force applied on the structural members. The force produced during fast switching has two components, one is in the tangential direction and the other is in the radial direction. The tangential component is related to the acceleration and the radial component is proportional to the square of the slewing rate. Therefore it is necessary to limit both acceleration and slewing rate during fast switching, particularly the slewing rate.

5.2 Structure admittance factor

For structures under external excitation, the structure response can be represented by the convolution of the spectrum density of the excitation with the admittance of the structure. The admittance of the structure is also called the dynamic magnification factor. This function is complex; it is related to the structural natural frequencies and the damping factors. However in the lower end of the spectrum, when the ratio between the frequencies of the excitation and the structural mode is smaller than 0.5, the admittance is near to unity (see Fig. 9 which is the admittance for a single mass spring system). Therefore the structure will have its displacement d = F/K, where F is outside force and K is the generalized structural stiffness. However, when the frequency of outside excitation is approaching the structure natural frequency, the admittance function of the structure will increase and have a sharp peak depending upon the damping factor. The smaller the damping factor is, the sharper its peak is. Therefore antenna structures should be designed to have their natural frequencies far away from the possible frequencies of excitations. For complex structure like antennas, there will be many sharp peaks on their admittance functions; these peaks all correspond to their natural frequency modes. Crosstalk between modes is not a significant issue for antenna structure.

5.3 The deformation of the dish surface

From the analysis, if the damping factor is 0.04, the maximum dish surface displacement 1 second after fast switching is within 100 microns for all three routines (the last two routines have smaller maximum displacements). Since the structural grid nodes vibrate at higher frequency than the integration, the recorded radiation is an average of all the deformed patterns. Although the estimated rms error for the whole dish at the maximum position is

larger than the required 25 microns, the average rms error will be within this requirement.

Damping factor for steel structure usually is 0.02, for CFRP the number is slightly higher. However, the antenna structure is highly complex and it has more joints and members. Although the expected damping factor is small, it should be near 0.04. Therefore, only minor damping is needed for the backup structure and the panel support.

5.4 Tripod vibration

Tripod vibration is the main reason which makes the fast switching very difficult. For a slant antenna structure, the tripod vibration mode is a dominant one in the natural frequency list. Even for the present tripod design, which is very stiff and has a larger blockage ratio, the secondary mirror still needs longer time to settle down to the required pointing accuracy(about 3 arc seconds). If no additional damping is applied, the secondary mirror will take 1.5 to 2 seconds to settle down for the present design at the uniform velocity routine. From Fig. 8, it can be found that a 0.06 damping factor is necessary to make the settling time within 1 second. By changing the control routine, the settling time can be reduced, but the gain from that is small; the gain by increasing the damping rate is more significant. A damping factor of 0.10 or over is preferred for the tripod structure.

The present tripod has an indirect blockage of about 8 %, which is too large. In order to reduce the aperture blockage, the tripod has to be redesigned. One option in reducing the aperture blockage is to use members with a small cross section, the other option is to adapt the traditional tripod design. In both cases, the stiffness of the tripod will be reduced and the natural frequency will be low. In order to satisfy the fast switching requirement, additional damping is necessary for the members of tripod. If the tripod is built by constrained layer structural members, its damping factor can be significantly large. Damping factors of 1.0 or larger can be achieved by applying this passive treatment.

5.5 Constrained layer damping design

The constrained layer member is formed by adding two thin layers of material on the top of the structure memeber. The middle layer of material is a viscoelastical one and the top layer is the same material as the structure member. The top layer sheet member is constrained at one end only. Therefore when the structure members are under periodical force, the shear loss of the energy within the viscoelastic layer will increase the structural loss factor greatly. The loss factor of the constrained layer member is expressed as:
where G_2 is the shear modulus of the viscoelastic material, E is the Youny's modulus of the structrual material, L, h and t are the member length, member thickness and the viscoelastic layer

$$\eta = \frac{\pi G_2 L^2}{3Eth}$$

thickness. Although G_2 of the viscoelastic material is about 1000 time less then E of the structure member, high L and t ratio will still make the loss factor significant. It is not difficult to design a constrained layer member with a damping factor as high as 0.50 or 1.0. Details about this damping method will be discussed in a separated memo.

6. Conclusion

The current slant axis design comes very close to satisfying the fast switching requirement for the MMA antennas; the antennas will be able to switch 1.5 degrees in 1 second of time, with a residual pointing error of less than 3 arc seconds. The performance is currently limited by the response of the secondary mirror support structure; this can be improved significantly by application of constrained layer damping. Deformations of the dish surface induced by fast switching are within acceptable limits. The interaction between the antenna servo system and the structure will be addressed in future work.

7. Acknowledgement

I am indebted to D. Emerson, J. Payne and R. Freund for help and many stimulating discussions throughout the computer simulation of the fast switching.

References

1. Nastran theorectical manual, MacNeal-Schwendle Corportion, 1972.

2. Fundamentals of automatic control, S. Gupta and L. Hasdorff, John Wiley & Sons, Inc., 1966.

3. The FFT Fundamentals and concepts, R. W. Ramirez, Prentice-Hall, Inc., 1985.

4. Structural vibration analysis, C.F. Beards, Ellis Horwood Ltd., 1983.

5. Damping applications for vibration control,Proc. of the annual meeting of the American society of mechanical Engineers, Chicago, Illinois, Nov. 16-21, 1980.

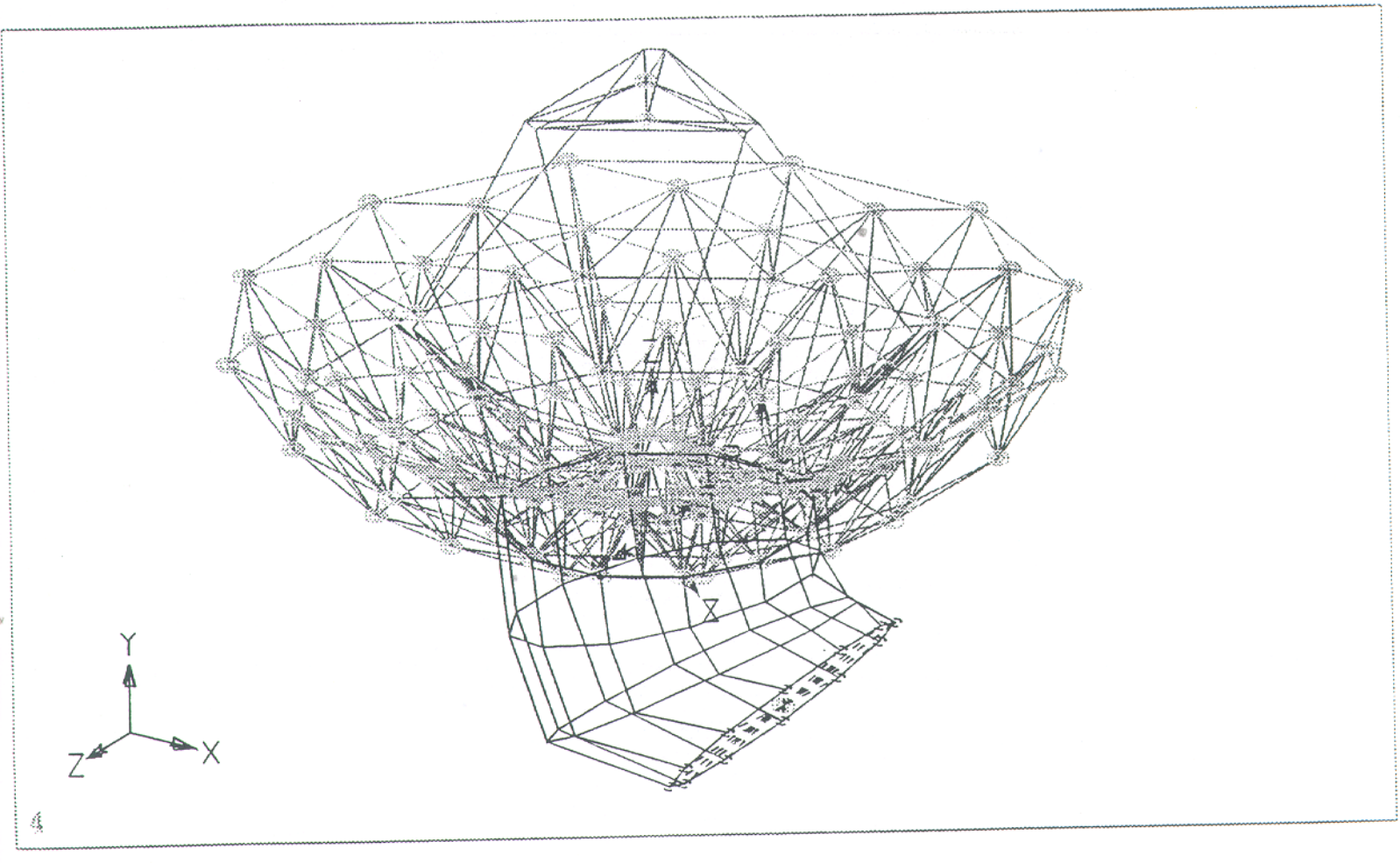

Figure 1 Perspective view of the transient analysis model.

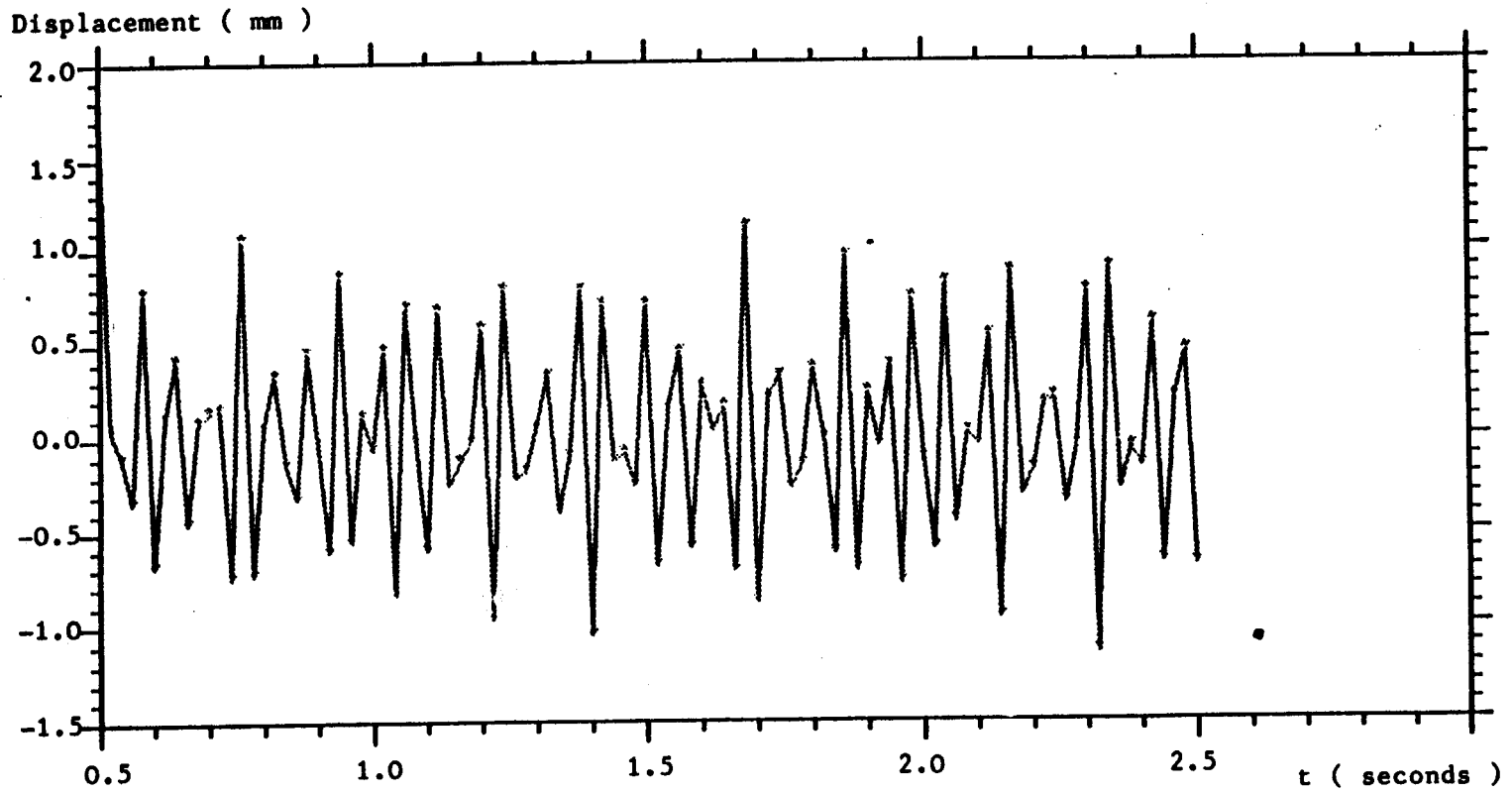

Figure 2 Displacement curves of dish surface edge node in z direction for switching routine one when damping factor is zero.

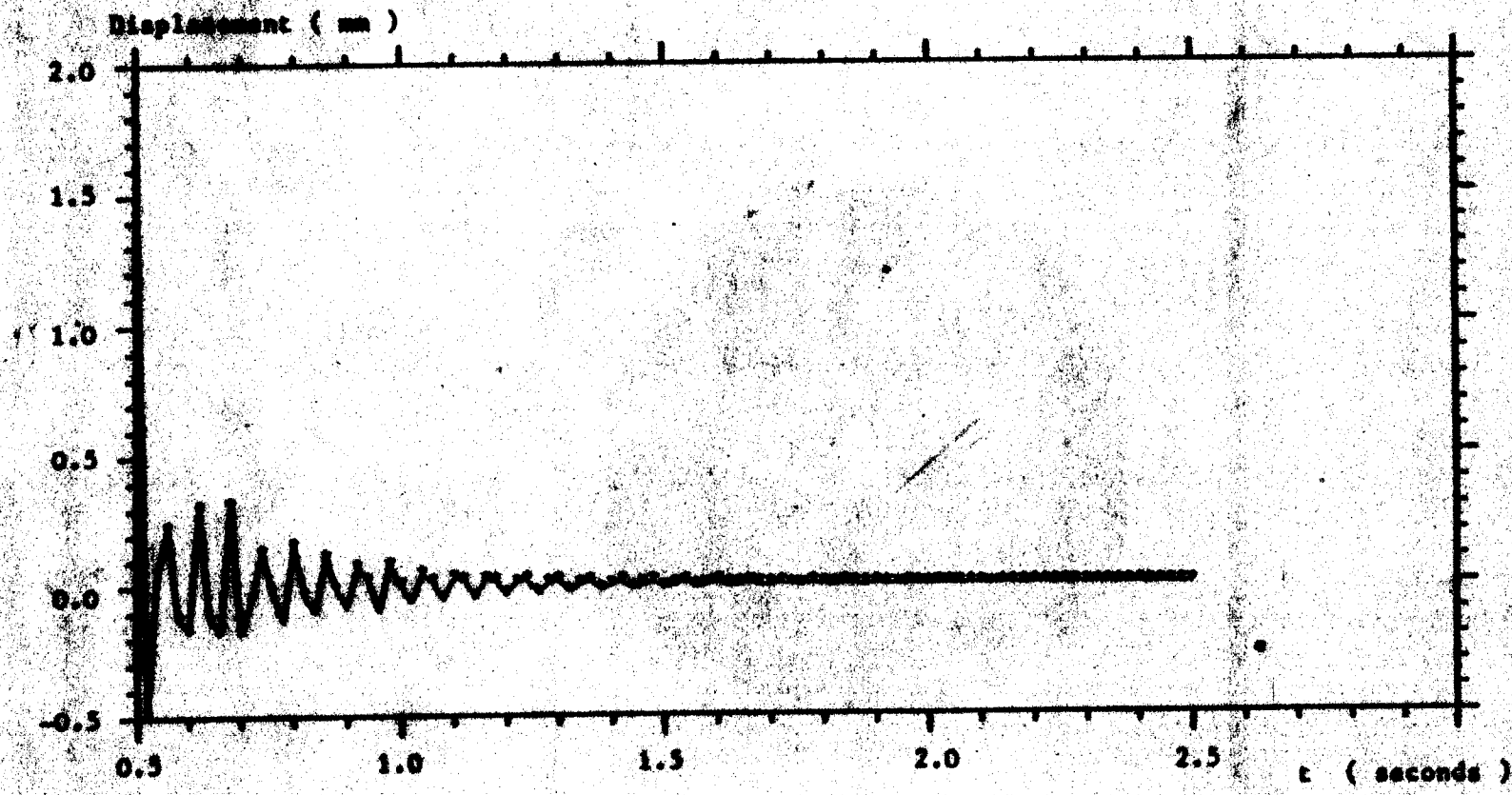

Figure 3a Displacement curve of dish surface edge node in z direction for switching routine one when damping factor is 0.04.

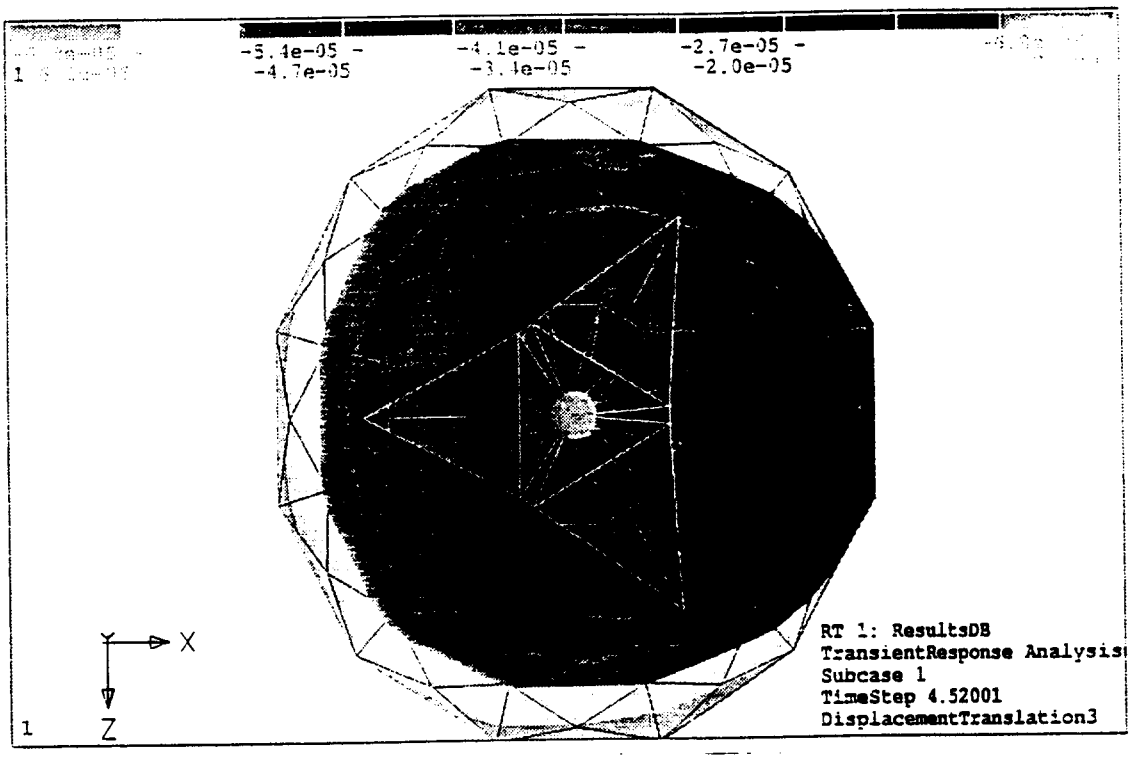

Figure 3b Dish surface contour map of peak displacements in z direction at t=1.02 seconds for switching routine one.

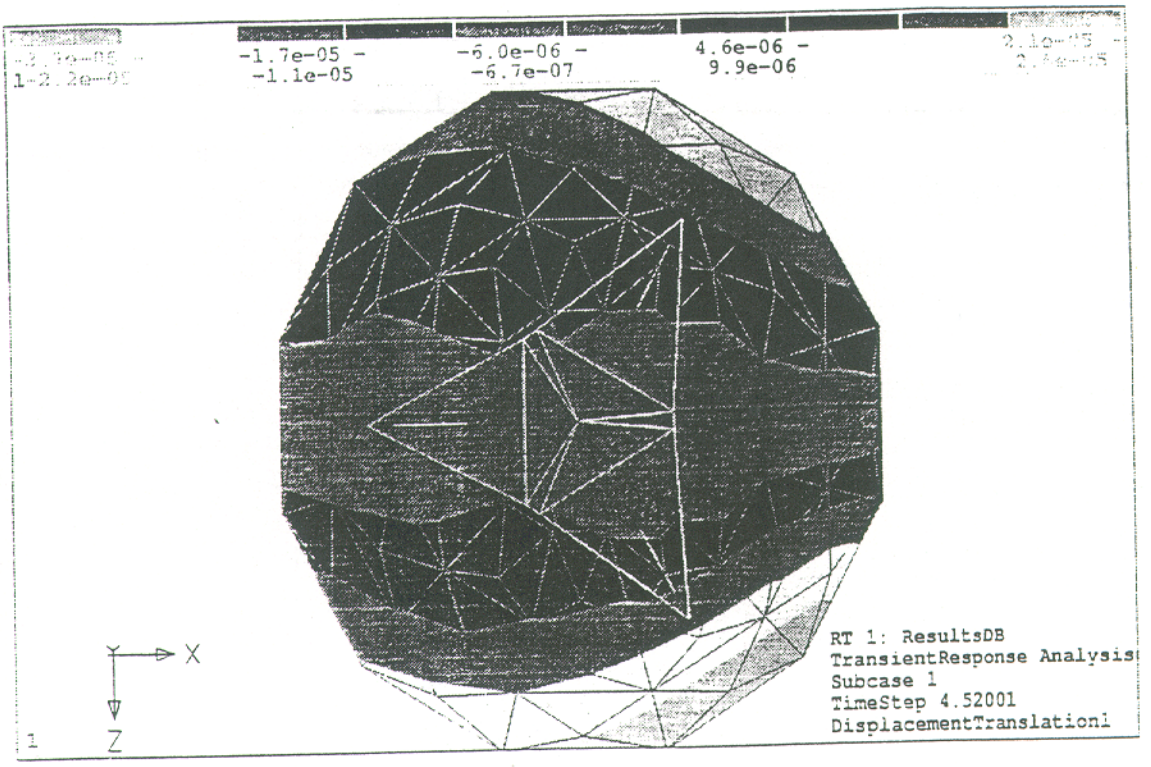

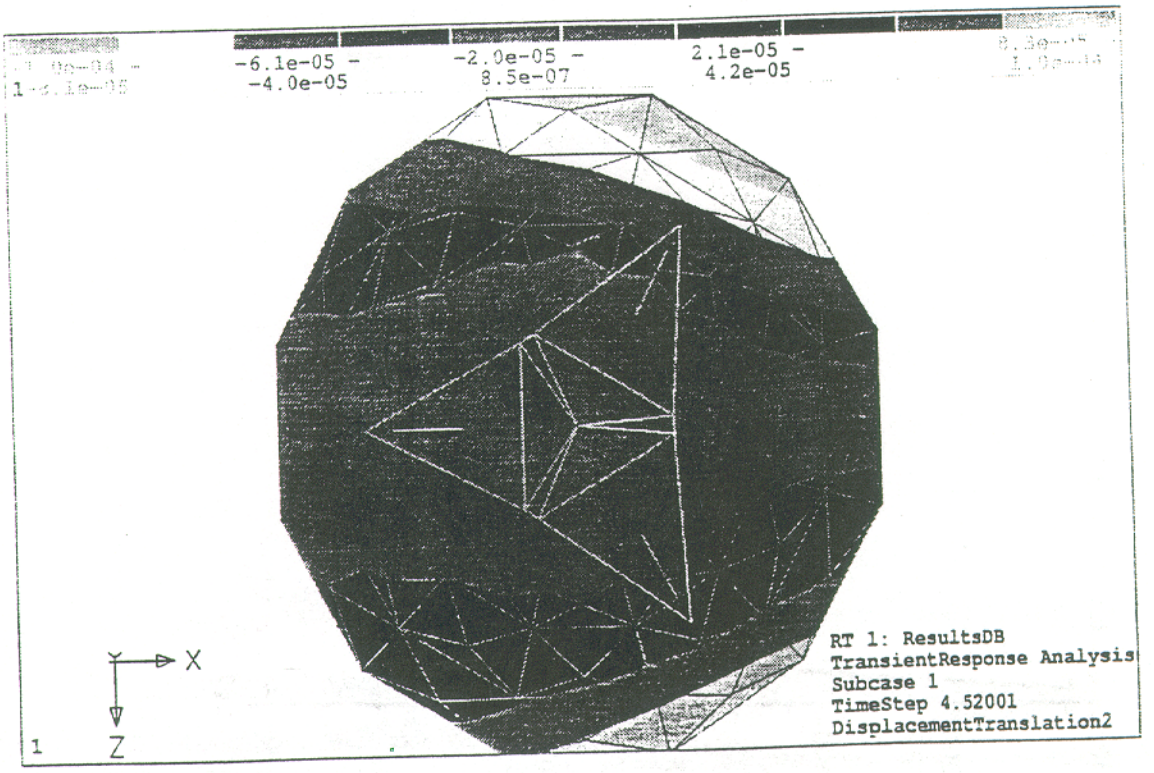

Figure 3c Dish surface contour map of peak displacements in x direction at t=1.02 seconds for switching routine one.

Figure 3d Dish surface contour map of peak displacements in y direction at t=1.02 seconds for switching routine one.

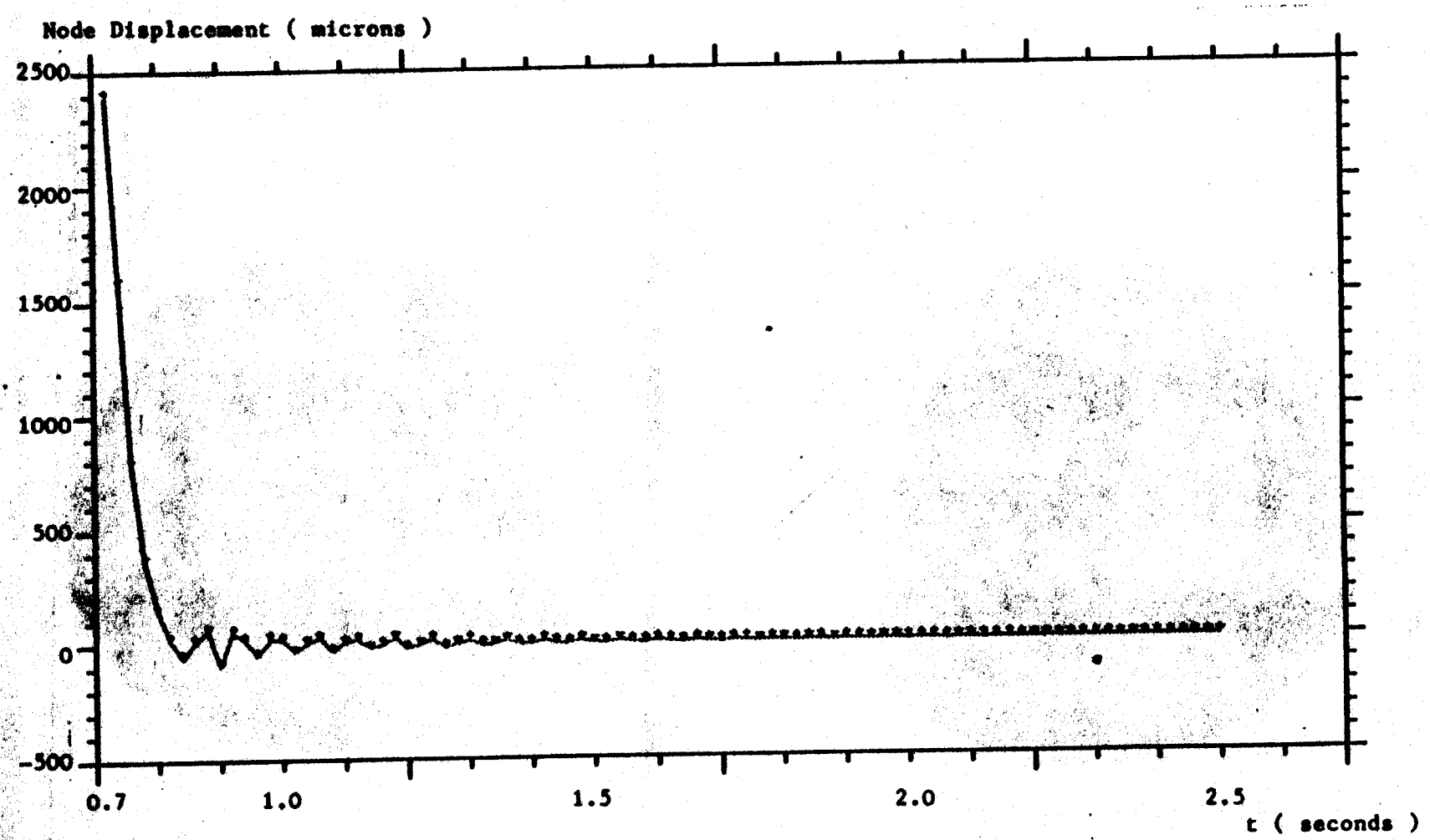

Figure 4 Displacement curves of dish surface edge node in z direction for switching routine two when damping factor is 0.04.

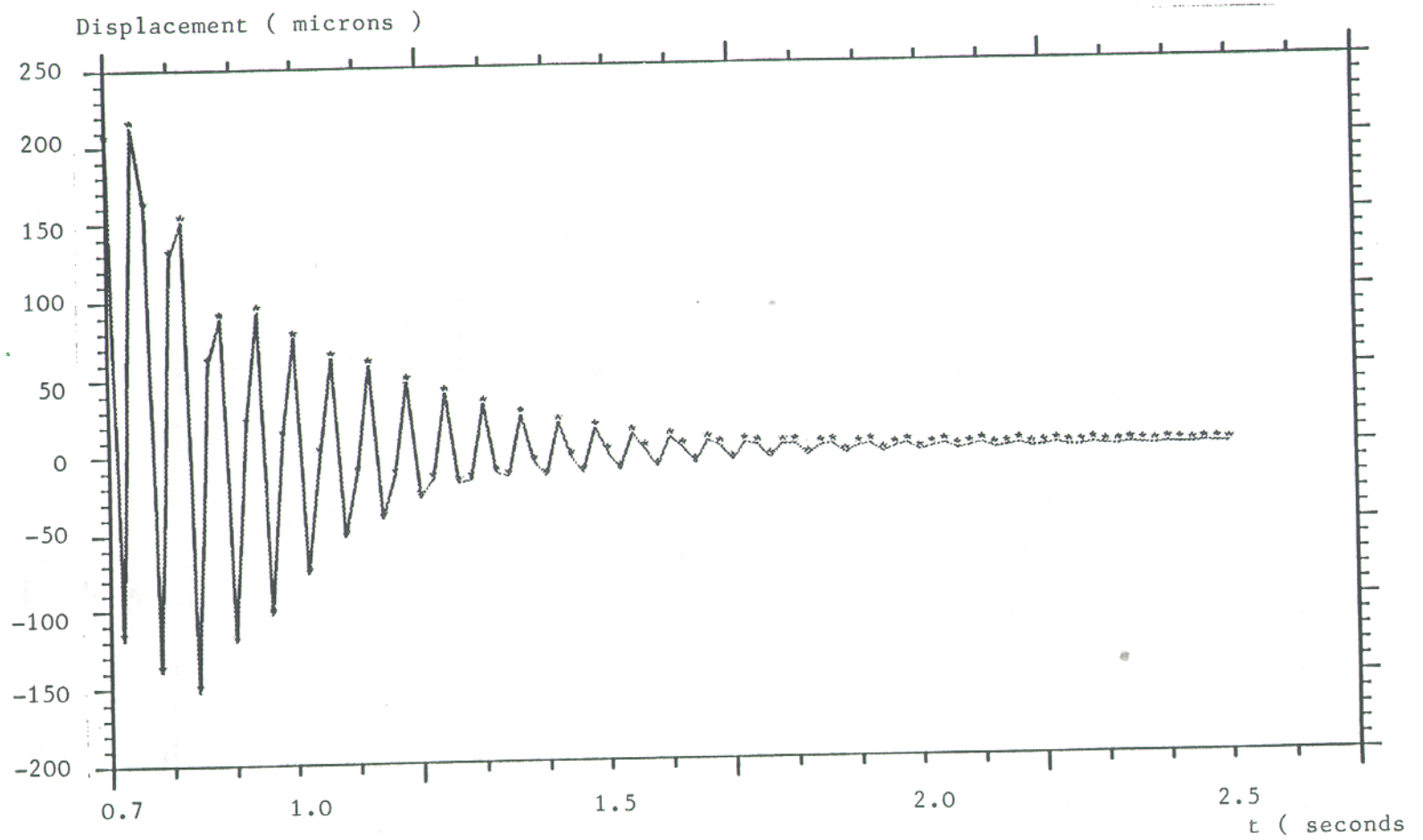

Figure 5 Displacement curves of dish surface edge node in z direction for switching routine three when damping factor is 0.04.

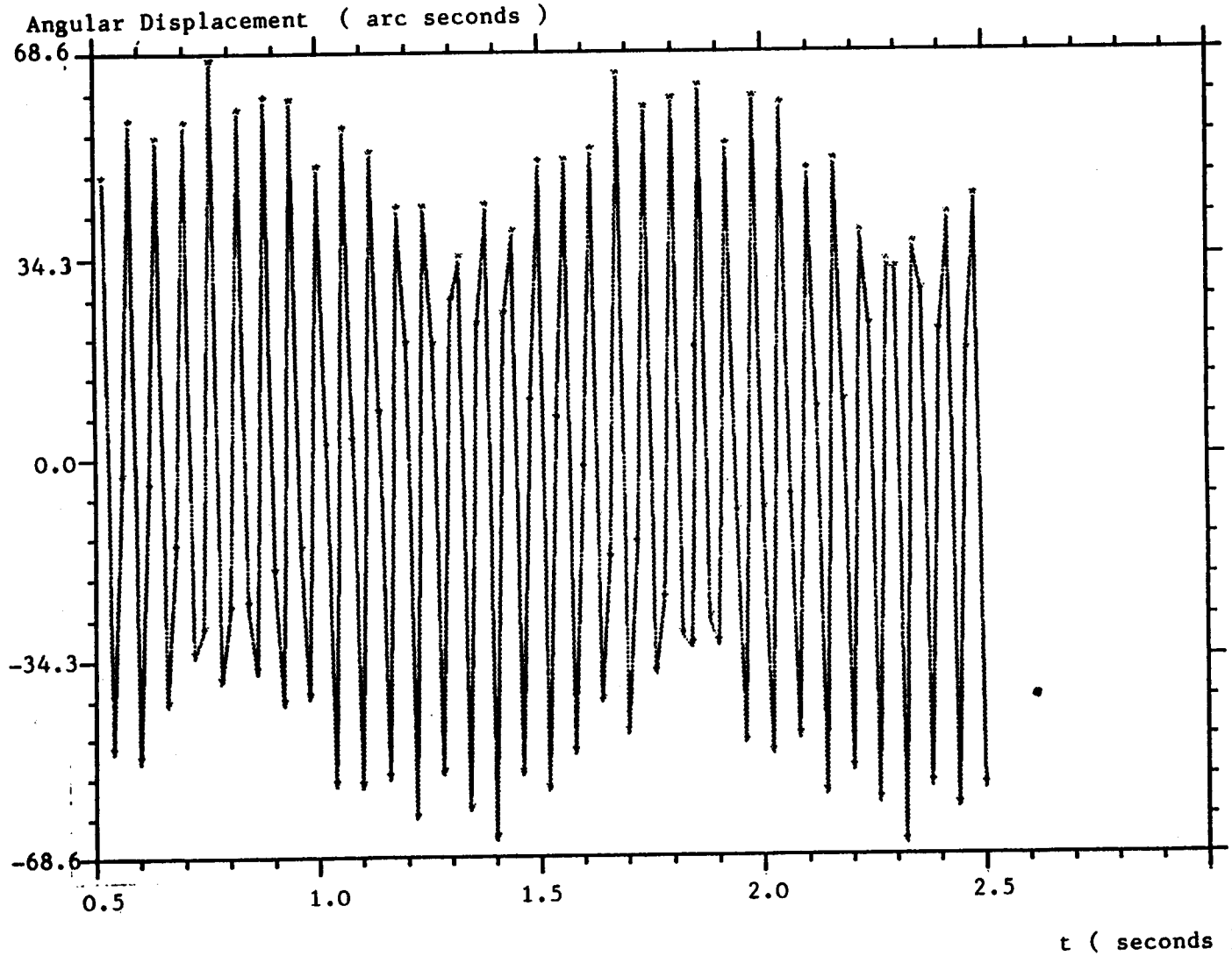

Figure 6 Displacement curve of the secondary mirror node in z direction for switching routine one when damping factor is zero.

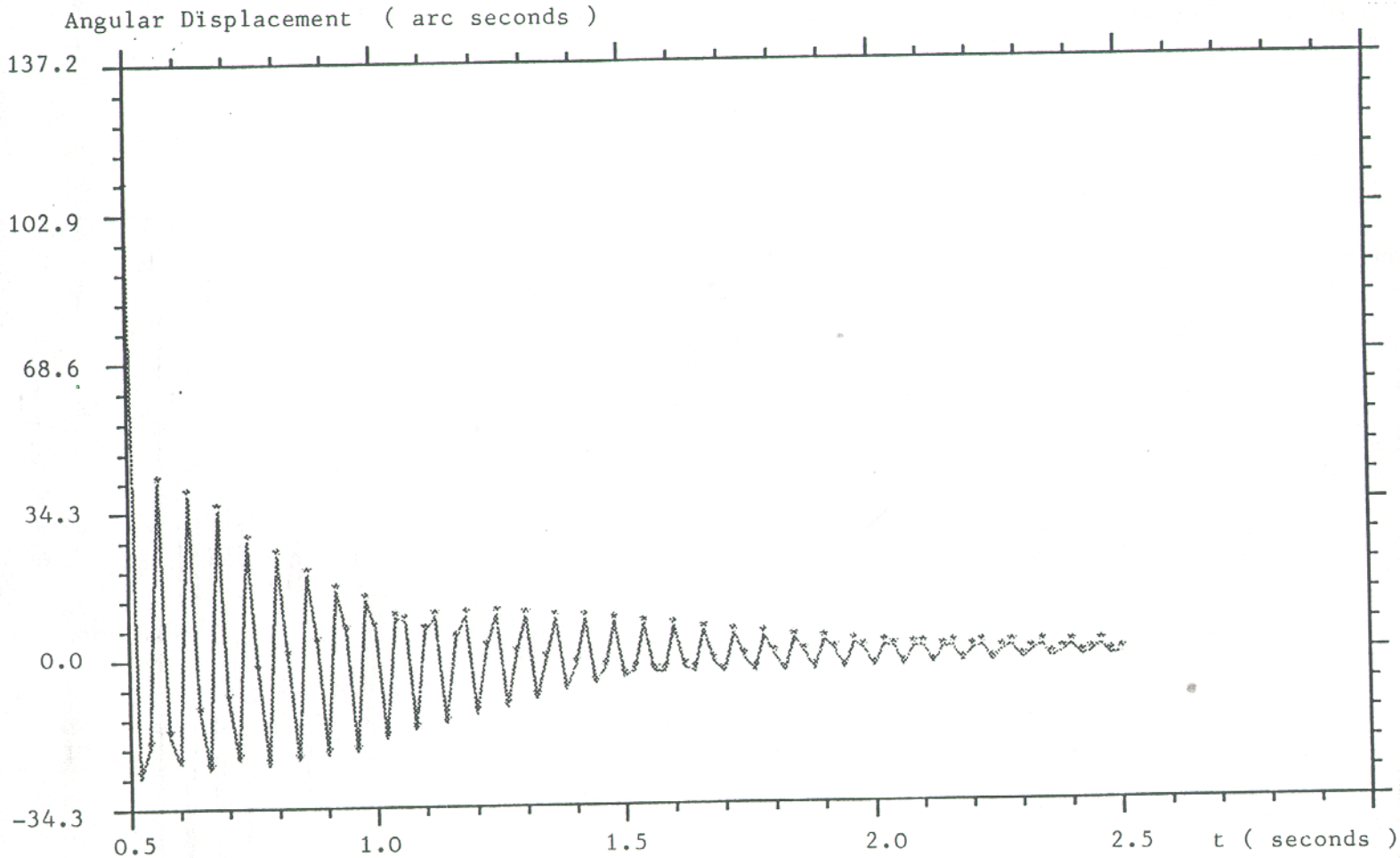

Figure 7a Details of the displacement curve of the secondary mirror node in z direction for switching routine one when damping factor is 0.02.

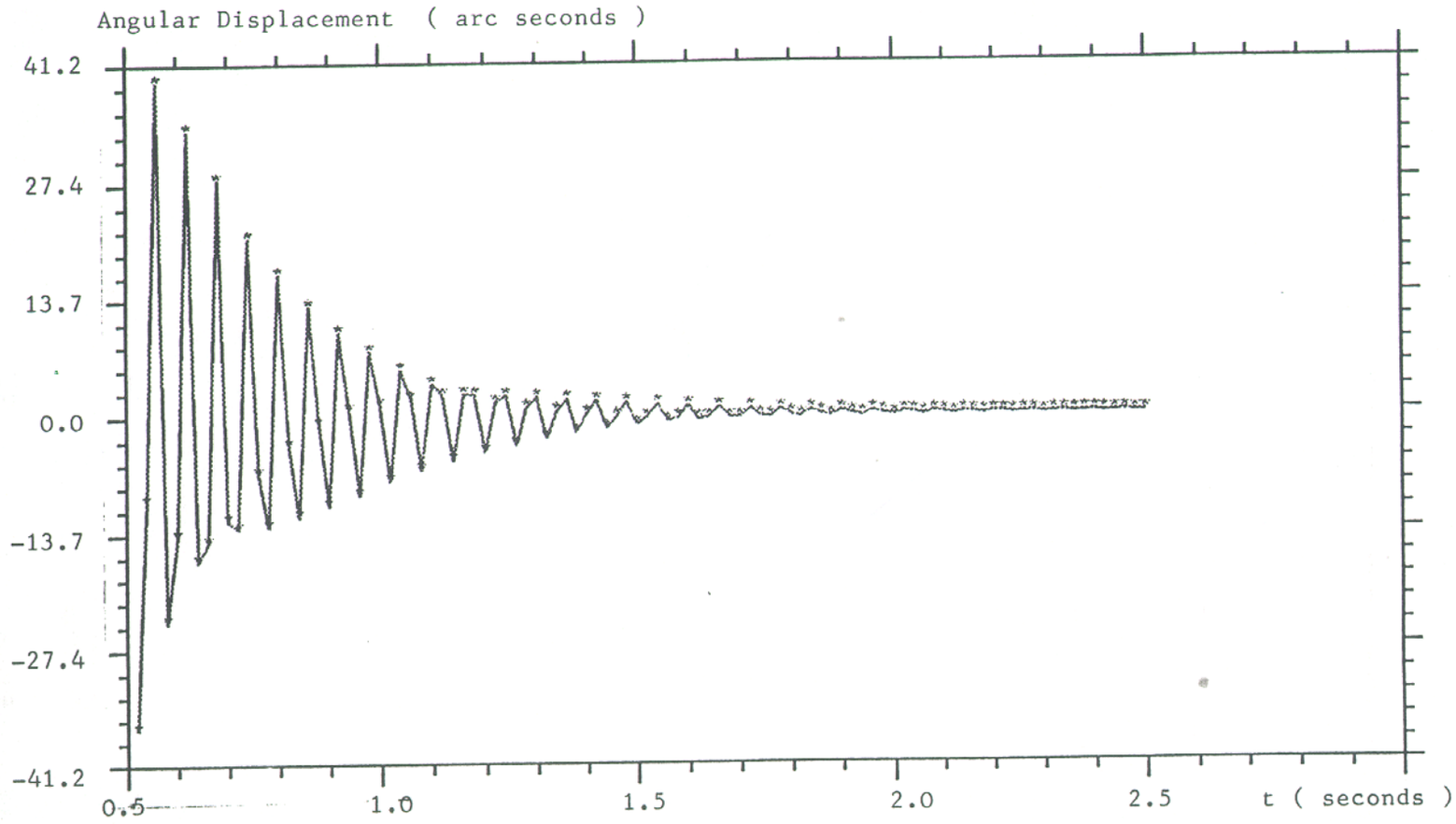

Figure 7b Details of the displacement curve of the secondary mirror node in z direction for switching routine one when damping factor is 0.04.

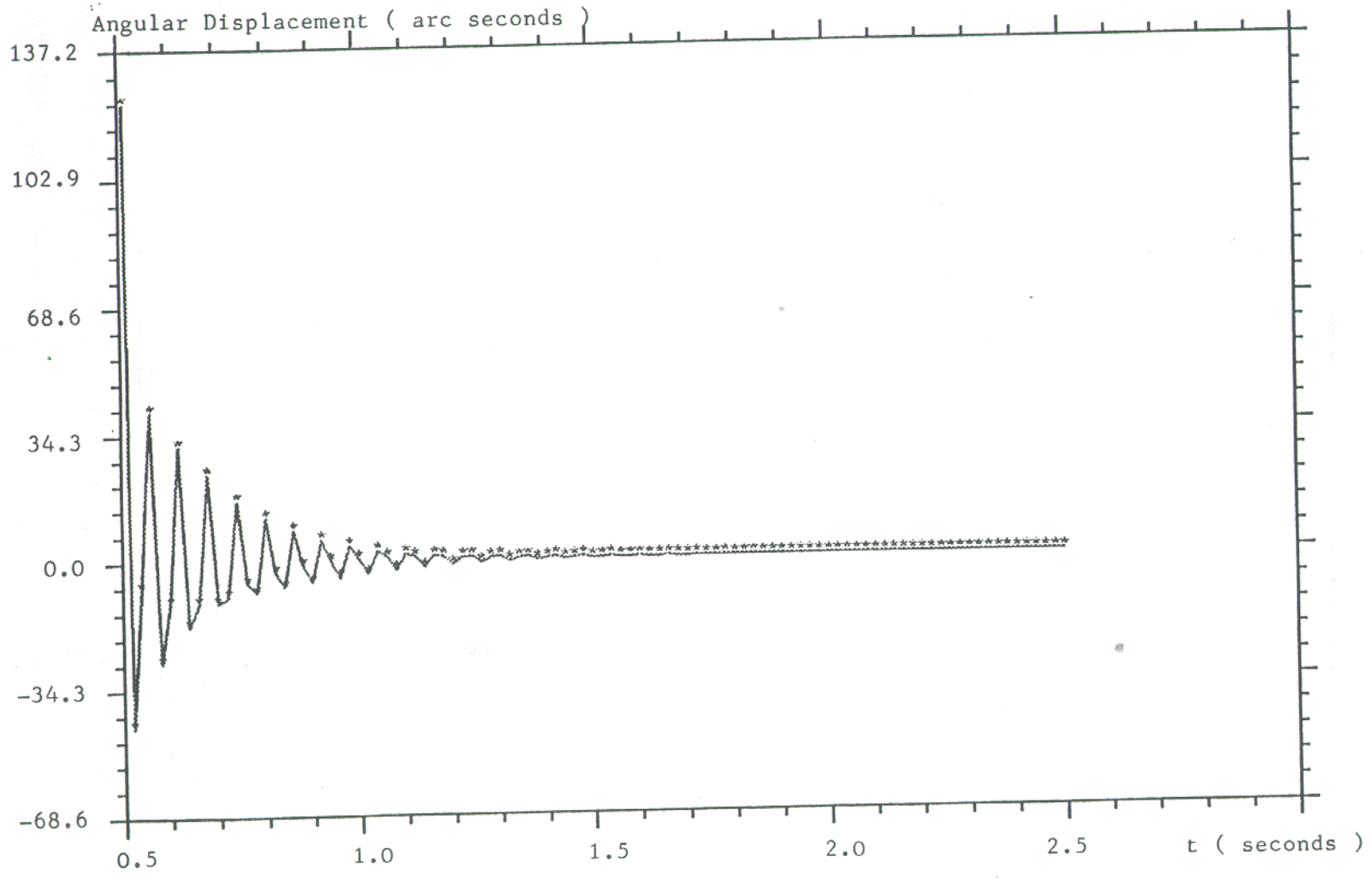

Figure 7c Details of the displacement curve of the secondary mirror node in z direction for switching routine one when damping factor is 0.06.

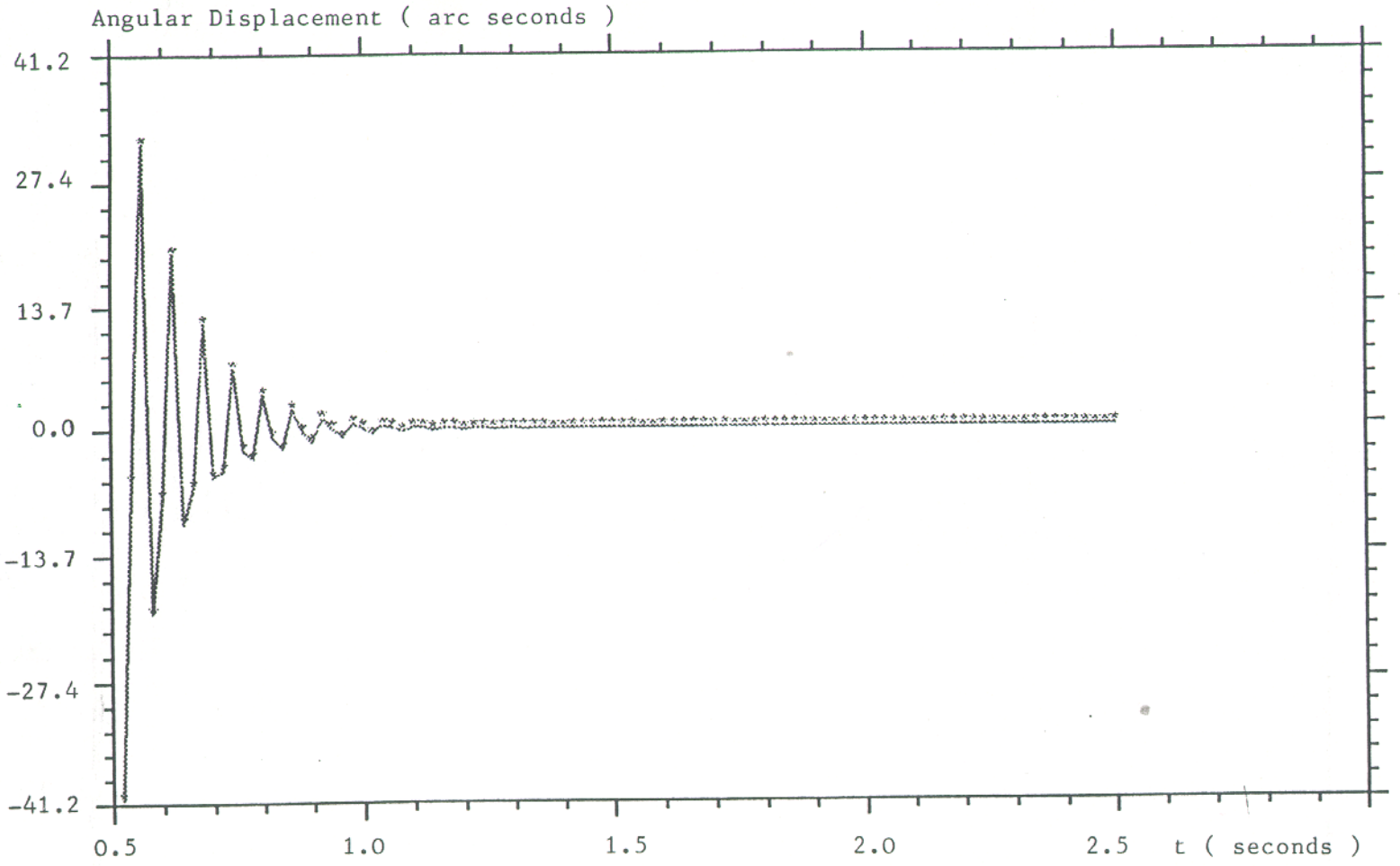

Figure 7d Details of the displacement curve of the secondary mirror node in z direction for switching routine one when damping factor is 0.1.

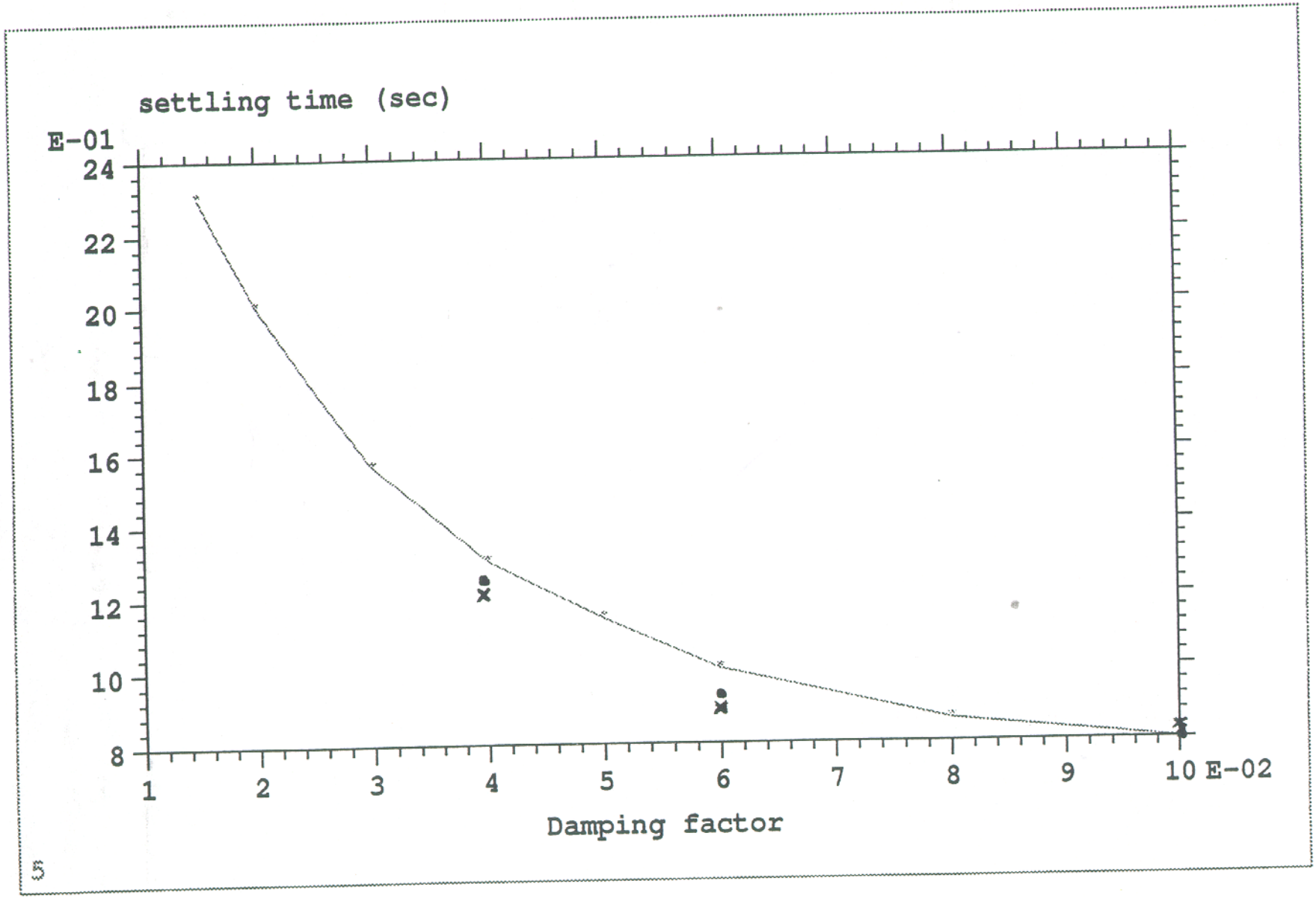

Figure 8 The relationship between damping factor and the settling time for secondary mirror node when switching routine is a uniform velocity one. In the figure, small dots represent those of switching routine two, small crosses represent those of switching routine three.

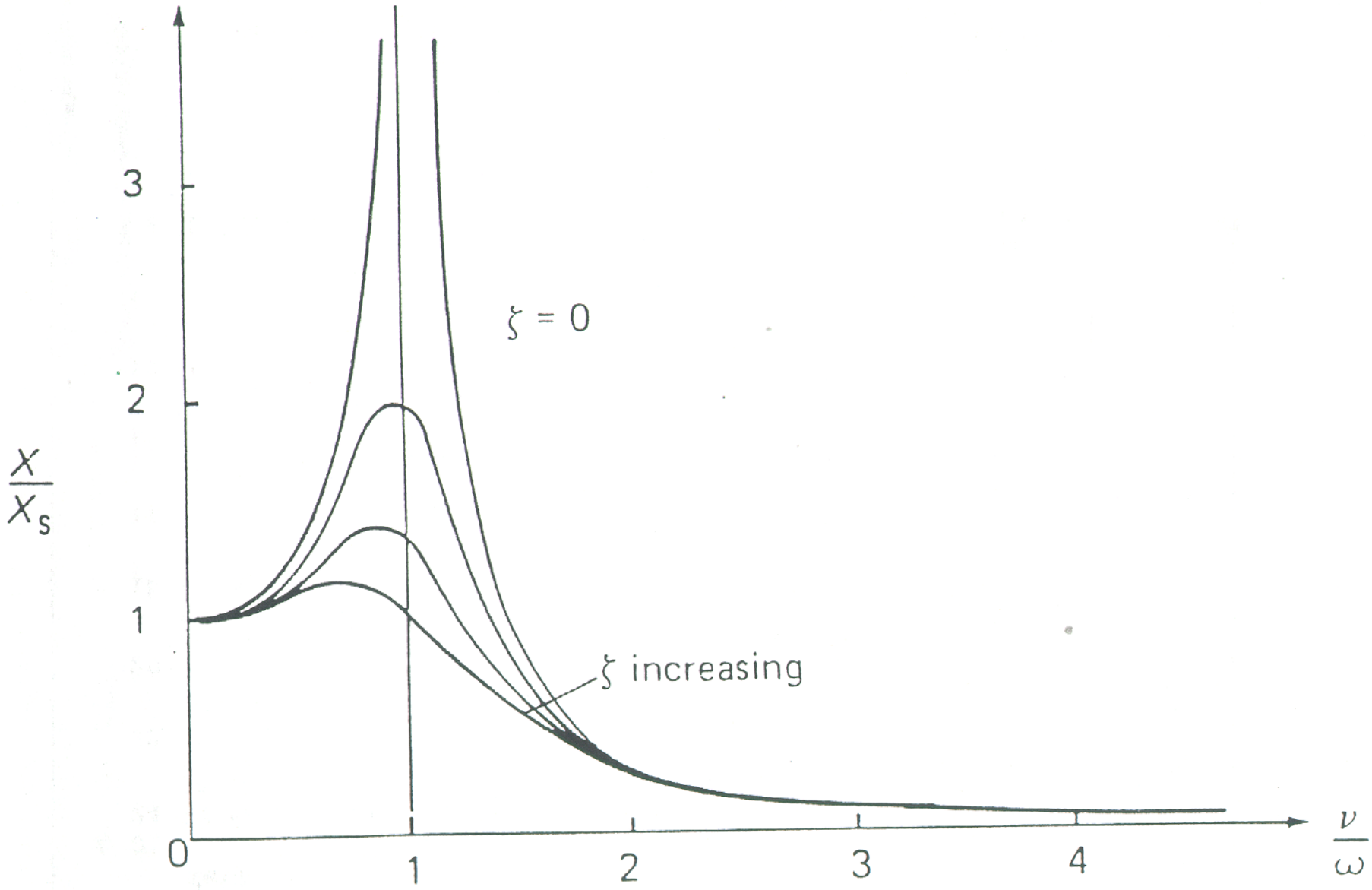

Figure 9 Structural admittance as a function of frequency ratio between excitation and structural modes.